

Supporting Information

White Light Emission and Superior Color Stability in a Single-Component Host with Exceptional Eminent Color Rendering and Theoretical Calculations on Duv for Color Quality

Wasim Ullah Khan^a, Waheed Ullah Khan^b, Haris Ziman^c, Ayaz Mahsud^d, Dilfaraz Khan^d, Salim Ullah Khan^e Shuakat Khan^f, and Yueli Zhang^{a*}

- a. School of Materials Science and Engineering, Sun Yat-sen University, Guangzhou 510275/Analysis and testing center, Shenzhen Technology University, Shenzhen, 518118 P. R. China*
- b. Institute for Advanced Study, and School of Physics and Optoelectronics Engineering, Shenzhen University, Shenzhen, 518060, PR China*
- c. School of Chemical Sciences, Peshawar University, Peshawar, Khyber Pakhtunkhwa, 29050, Pakistan*
- d. Institute of Chemical Sciences, Gomel University, Dera Ismail Khan, Khyber Pakhtunkhwa, 29050, Pakistan*
- e. University of Science and Technology Bannu, Khyber Pakhtunkhwa, 29050, Pakistan*
- f. Department of Chemical Engineering, College of Engineering, Dhofar University, Salalah 211, Sultanate of Oman.*

Corresponding Author

*Email: stszyl@mail.sysu.edu.cn (Yueli Zhang)

Measurements and Characterizations

The powder X-ray diffraction (XRD) tests were conducted using a D8 X-ray diffraction system employing Cu K α radiation ($\lambda = 1.5418 \text{ \AA}$) at 35 kV and 35 mA. Optical microscope images were captured utilizing the KL 2500 LCD (feica). The sample morphologies were assessed using a JEOL 840A field emission scanning electron microscope (FE-SEM) with X-ray energy diffraction spectroscopy (EDAX) capabilities. For Transmission Electron Microscope (TEM) analysis, Selected Area Electron Diffraction (SAED), and element mapping, an FEI Tecnai G2 F300 instrument was employed. The examination of photoluminescence emission (PL) and excitation (PLE) spectra, as well as fluorescence lifetime, was carried out using the FLS920 Fluorescence Time-Resolved and Steady-State Spectrometer (Edinburgh Instruments) equipped with an Xe lamp and flash lamp. The temperature during measurements ranged from 300 K to 500 K and was regulated using a temperature controller. The quantum efficiency of the sample was measured using a Horiba FL3 (Japan) instrument equipped with an integrating sphere.

Supplementary Figures and Tables

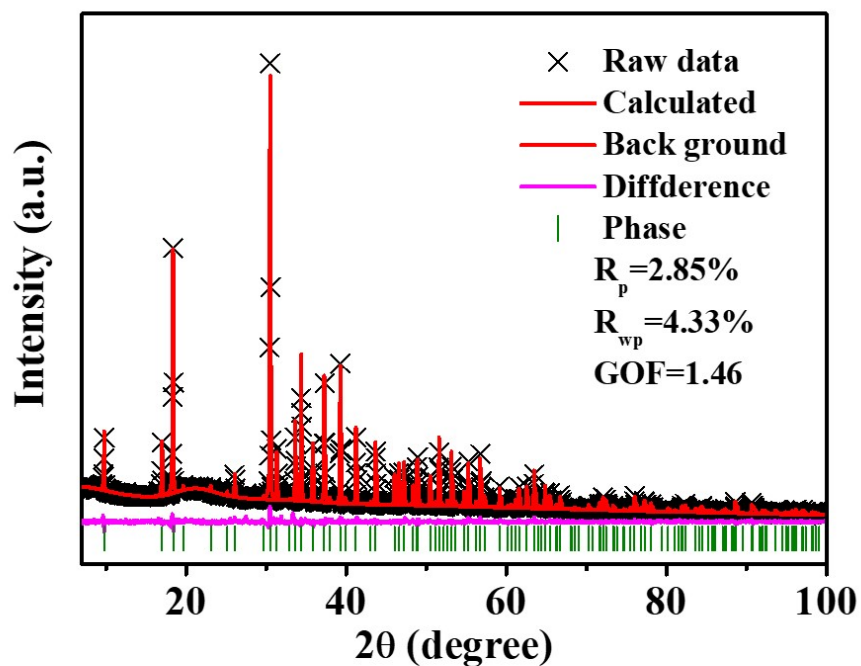


Fig. S1. Rietveld refinement result of the CYAB:0.08Dy³⁺ phosphor.

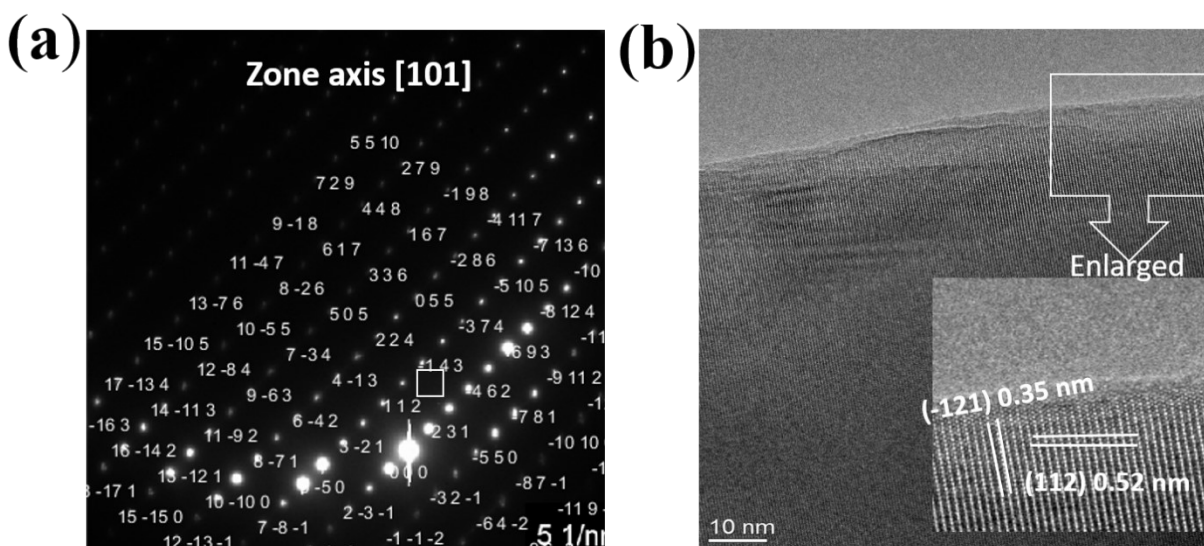


Fig. S2. The SAED, HRTEM of CYAB:0.08Dy³⁺ phosphor.

The XPS measurements (**Fig. 3**) provided additional evidence regarding the elemental composition. Analysis of the XPS spectra revealed specific peaks corresponding to various elements: C1s at 284.5 eV, O1s at 530.7eV, Ca2p_{1/2} at 347.55 eV, and Ca2p_{3/2} at 351eV. Additionally, peaks attributed to Al2p and B1s appeared at 71.55 eV and 188 eV, respectively. Y2p peaks were observed at 395.95 eV, 399.91 eV, and 403.55 eV. Moreover, distinctive peaks for Tm³⁺ were detected at 1063.8 eV for 3d_{5/2} and 1120.4 eV for 3d_{3/2}. Similarly, Dy³⁺ exhibited peaks at 1134.2 eV for 3d_{5/2} and 1170.1 eV for 3d_{3/2} [31]. These observations in the XPS spectra provide further confirmation of the elemental composition within the material.

Diffuse Reflectance Spectra

The energy band gap (E_g) of Ca₃Y₅Al₃B₄O₁₅, Ca₃Y₅Al₃B₄O₁₅:0.015Tm³⁺ and Ca₃Y₅Al₃B₄O₁₅:0.08Dy³⁺ is typically determined using the diffuse reflectance spectra (DRS) via the Kubelka-Munk function.[6, 7] The calculation involves the formula:

$$[F(R_{\infty})hv]^n = A(hv - E_g) \quad (S1)$$

Where A is a constant, hv represents the photon energy, E_g is the band gap, and n=1/2 indicates an indirect transition while n=2 signifies a direct transition. The Kubelka-Munk function, denoted as F(R_∞), is defined by

$$F(R_{\infty}) = \frac{A(1 - R)}{2R} = K/S \quad (S2)$$

Here, K, R, and S represent the reflections, the scattering coefficient, and the absorption, respectively. The estimated value of E_g is approximately 5.13 eV, derived from the linear extrapolation of $[F(R_{\infty})hv]^2 = 0$.

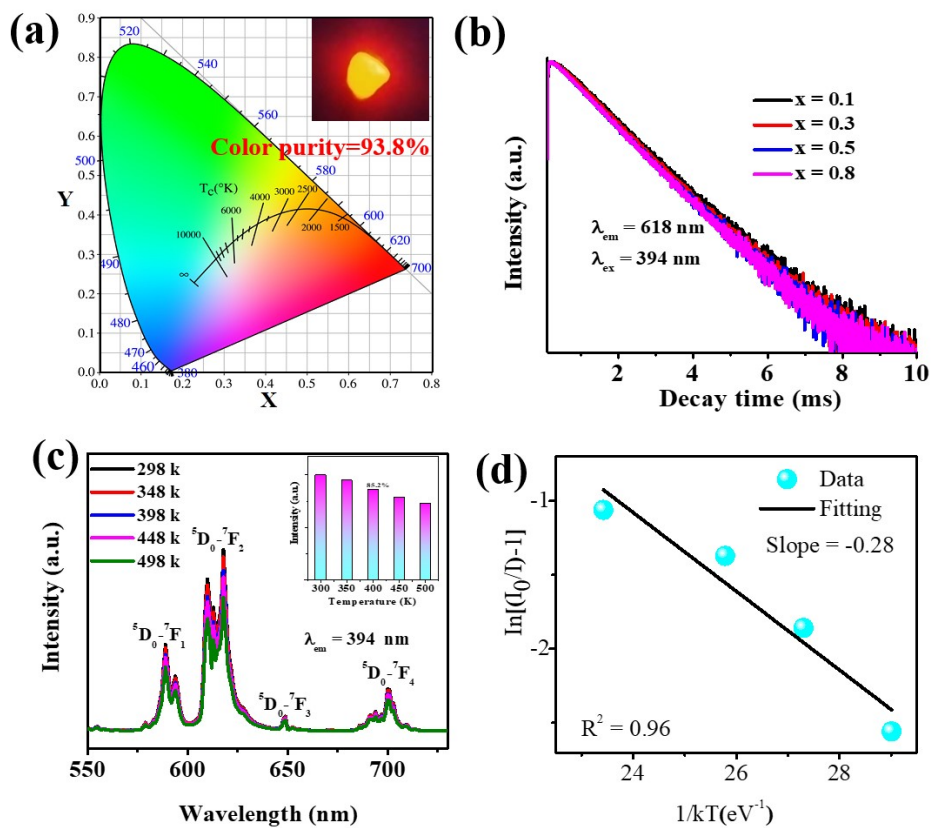


Fig. S3. (a) CIE diagram (inset image and color purity of the prepared phosphor). (c) Decay curve of CYAB:xEu³⁺. Temperature-dependent emission spectra and related PL intensity and modified Arrhenius fitting result of CYAB:Eu³⁺.

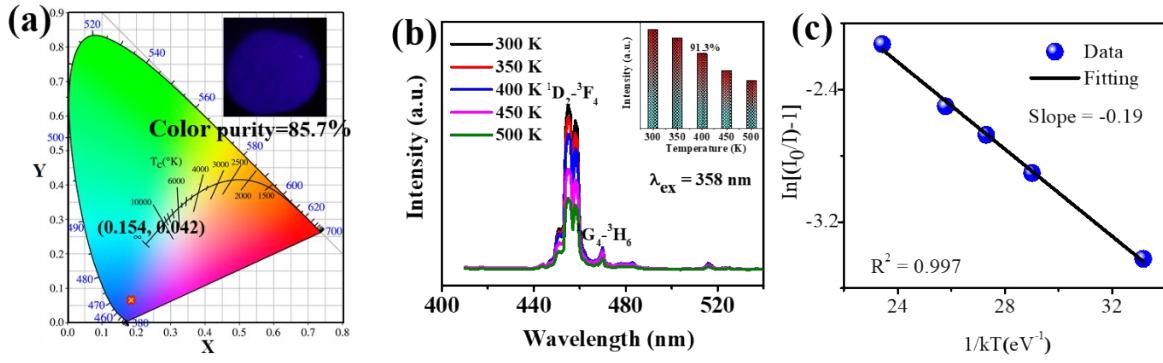


Fig. S4. (a) CIE diagram and color purity of the $\text{Ca}_3\text{YAl}_3\text{B}_4\text{O}_{15}:0.015\text{Tm}^{3+}$. (b) Temperature-dependent luminescence intensity and (c) The modified Arrhenius fitting result of $\text{Ca}_3\text{YAl}_3\text{B}_4\text{O}_{15}:0.015\text{Tm}^{3+}$.

Certainly, the decline in emission of CYAB:Eu^{3+} and CYAB:Tm^{3+} with increasing temperature is notable, where the integrated intensity at 400 K retains approximately 85.2% and 86.3% of its initial intensity at 303 K, respectively. To model these thermal quenching effects, the activation energy was estimated by applying the modified Arrhenius equation [6].

$$\frac{I_T}{I_0} = \left[1 + C \exp\left(\frac{\Delta E}{kT}\right) \right]^{-1} \quad (\text{S3})$$

The thermal quenching (ΔE) was estimated using the modified Arrhenius equation, where I_0 represents the original emission intensity, I_T is the intensity at various measuring temperatures T , C is a constant specific to the host material, k is the Boltzmann constant, and ΔE denotes the activation energy for thermal quenching. In this case, the thermal quenching (ΔE) has been calculated to be 0.28 eV for one scenario and 0.19 eV for another.

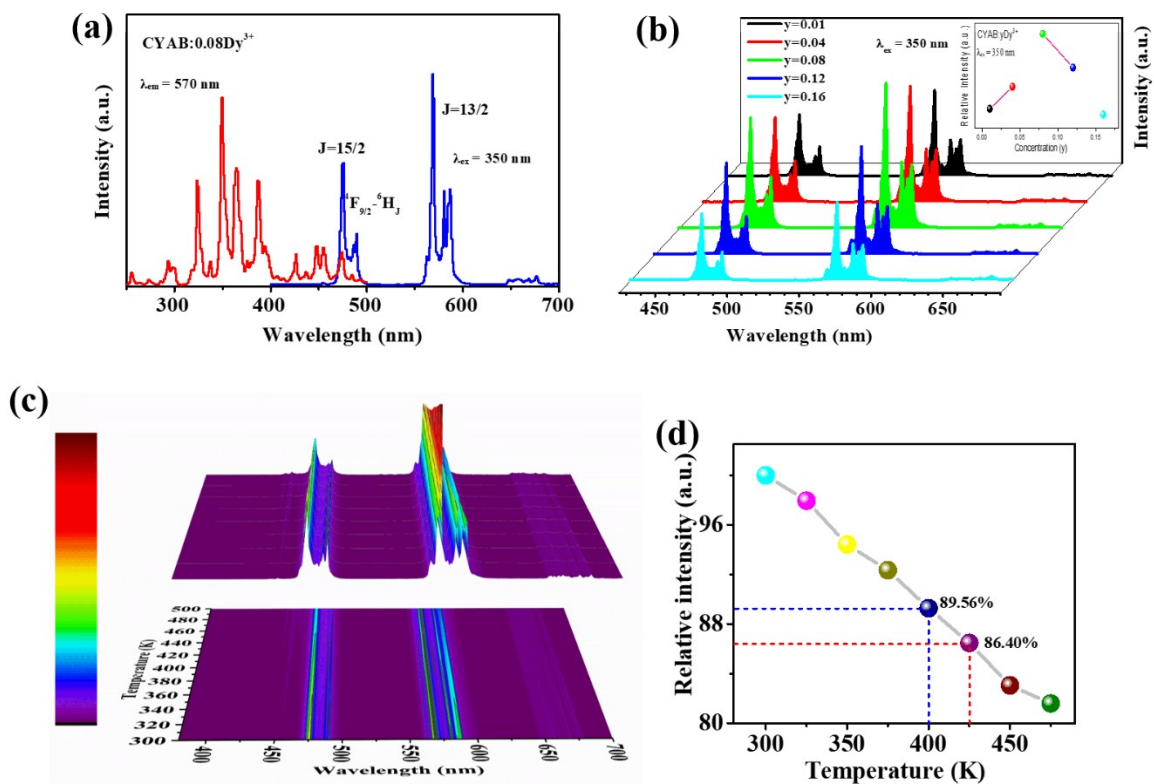


Fig. S5. (a) PLE and PL spectra of $\text{Ca}_3\text{YAl}_3\text{B}_4\text{O}_{15}:0.08\text{Dy}^{3+}$. (b) Concentration-dependent luminescence intensity of $\text{Ca}_3\text{YAl}_3\text{B}_4\text{O}_{15}:\text{xDy}^{3+}$. (c-d) The temperature-dependent PL spectra of $\text{Ca}_3\text{YAl}_3\text{B}_4\text{O}_{15}:\text{xDy}^{3+}$ and intensities of Dy^{3+} as the temperature variation.

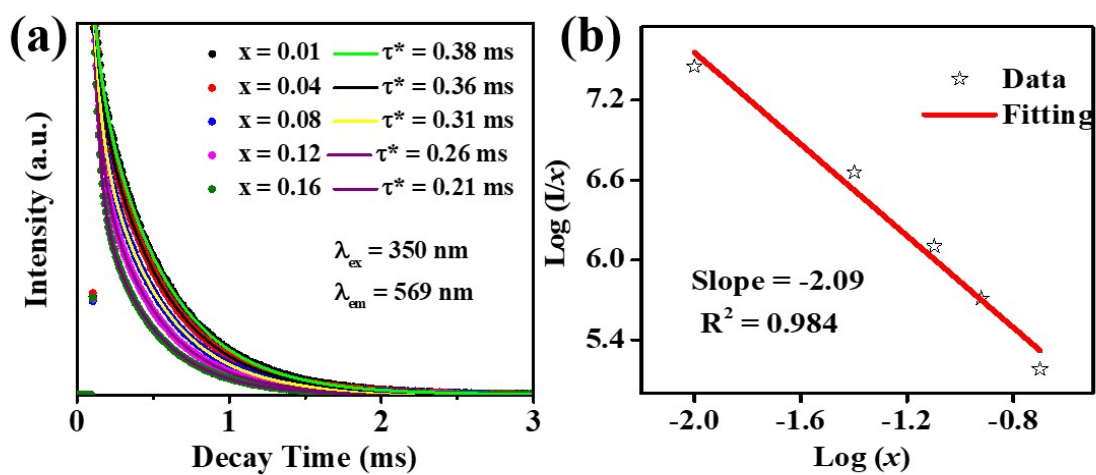


Fig. S6. (a) Decay curves, and (b) linear relationship of $\log(I/x)$ vs $\log(x)$ of the $\text{Ca}_3\text{YAl}_3\text{B}_4\text{O}_{15}:\text{xDy}^{3+}$.

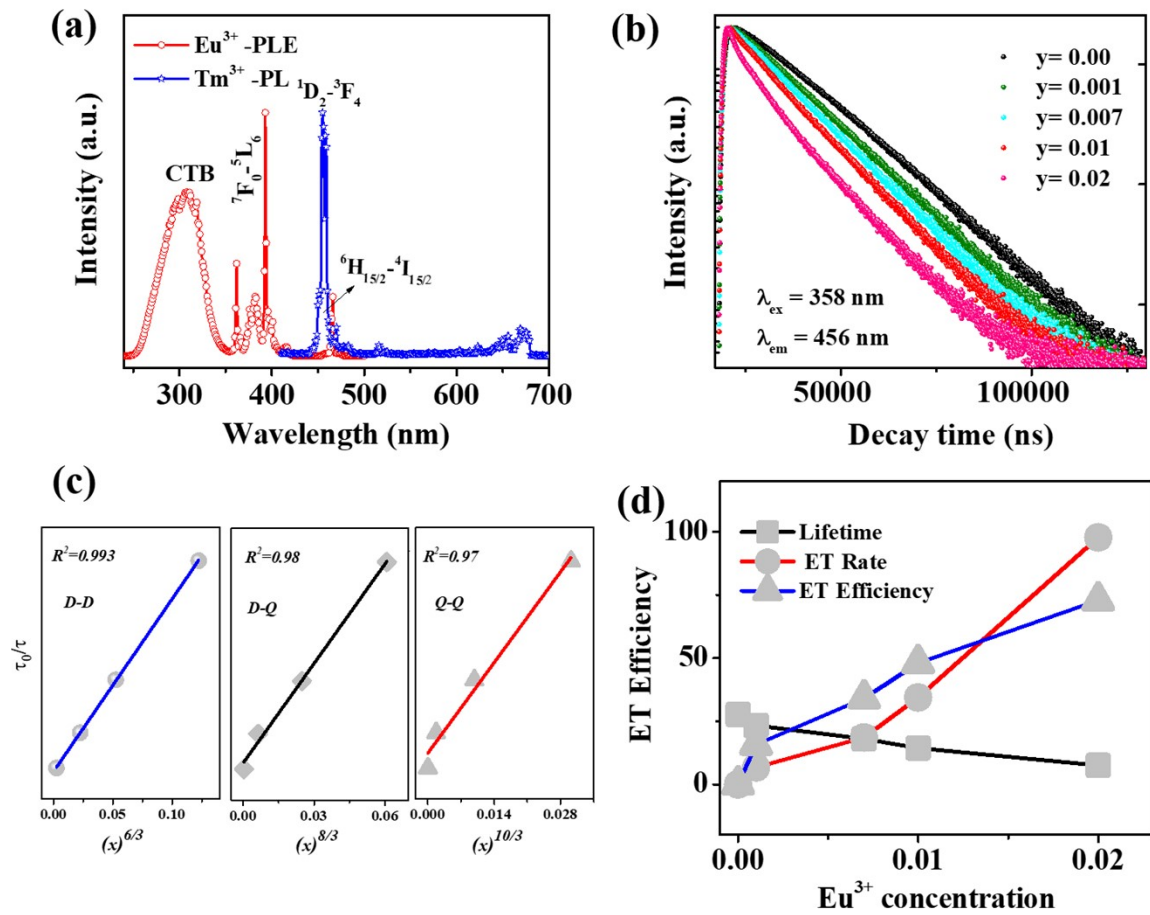


Fig. S7. (a) The spectral overlap of Eu^{3+} excitation and Tm^{3+} emission in $\text{Ca}_3\text{YAl}_3\text{B}_4\text{O}_{15}$. (b) Decay plot of $\text{Ca}_3\text{YAl}_3\text{B}_4\text{O}_{15}:\text{0.015Tm}^{3+},\text{0.08Dy}^{3+},x\text{Eu}^{3+}$ ($y=0.00, 0.001, 0.007, 0.01, 0.02$). The dependence of τ_0/τ on the total content of Tm^{3+} and activator in $\text{Ca}_3\text{YAl}_3\text{B}_4\text{O}_{15}$. (d) The lifetime, ET rate ($k_{\text{ET}} = 1/\tau - 1/\tau_0$), and $\eta = 100(1 - \tau/\tau_0)$ as a function of Eu^{3+} contents.

Table-S1. Fractional Atomic Coordinates and Equivalent Isotropic Displacement Parameters (\AA^2) for $\text{Ca}_3\text{YAl}_3\text{B}_4\text{O}_{15}:\text{M}$ ($M=\text{Dy}$)

Atoms	Site	X	Y	z	U_{iso}	N
Ca1/Y1	2c	0.333/0.333	0.666/0.666	0.250/0.250	0.00(13)	0.00/0.00(14)
Ca2/Y2	6h	0.128/128(5)	0.840/0.840(5)	0.250/0.250	0.99(2)	0.97/0.12(5)
Al	6g	0	$\frac{1}{2}$	0	0.0160(15)	1
B1	6h	0.2168(3)	0.7636(3)	$\frac{3}{4}$	0.004(5)	1
B2	4e	0	0	-0.0899(12)	0.04(2)	$\frac{1}{2}$
O1	12i	0.3407(13)	0.9233(12)	$\frac{1}{4}$	0.016(4)	1
O2	12i	0.3006(2)	0.4660(14)	0.5369	0.019(4)	1
O3	6h	-0.0435(9)	0.1037(8)	0.4071(12)	0.010(2)	1
O4	6h	0.08261(3)	0.4637(3)	0.2500(3)	0.016(4)	1

Space group $P63/m$: $a = b = 10.3855(6)$ \AA , $c = 5.6911(4)$ \AA , Reliability factor: $R_p = 0.0285$, $R_{\text{wp}} = 0.0421$.**Table S2.** CIE chromaticity coordinates of $\text{Ca}_3\text{YAl}_3\text{B}_4\text{O}_{15}:\text{0.015Tm}^{3+},\text{0.08Dy}^{3+},\text{xEu}^{3+}$ phosphors under 358 and 361 nm excitation

Samples	Excitation	CIE (x, y)	CCT (kelvin)
CYAB:0.015Tm ³⁺ ,0.08Dy ³⁺ ,0.001Eu ³⁺	358 nm	(0.316, 0.322)	6543
CYAB:0.015Tm ³⁺ ,0.08Dy ³⁺ ,0.007Eu ³⁺	358 nm	(0.319, 0.326)	5909
CYAB:0.015Tm ³⁺ ,0.08Dy ³⁺ ,0.01Eu ³⁺	358 nm	(0.322, 0.329)	5789
CYAB:0.015Tm ³⁺ ,0.08Dy ³⁺ ,0.02Eu ³⁺	358 nm	(0.326, 0.332)	5329
CYAB:0.015Tm ³⁺ ,0.08Dy ³⁺ ,0.001Eu ³⁺	361 nm	(0.346, 0.324)	4635
CYAB:0.015Tm ³⁺ ,0.08Dy ³⁺ ,0.007Eu ³⁺	361 nm	(0.360, 0.324)	3406
CYAB:0.015Tm ³⁺ ,0.08Dy ³⁺ ,0.01Eu ³⁺	361 nm	(0.381, 0.328)	3065
CYAB:0.015Tm ³⁺ ,0.08Dy ³⁺ ,0.02Eu ³⁺	361 nm	(0.426, 0.332)	2239

Table-S3. Lifetimes, fitting Parameters, energy transfer rates, and energy transfer efficiency for CYAB:0.015Tm³⁺,0.08Dy³⁺,xEu (x = 0 to 0.3) from measurements of Eu³⁺ emission at RT.

Dy ³⁺	R ² _{adj}	τ*	k _{ET} (ms) ⁻¹	η (%)
0	0.994	27.70	0.00	0.0
0.001	0.996	23.34	6.74	15.74
0.007	0.999	18.03	18.57	34.09
0.01	0.991	14.39	34.42	48.07
0.02	0.992	7.50	97.58	72.92

Table-S4 Calculated D_{uv} value of color quality and chromaticity shift (ΔE) of Ca₃YAl₃B₄O₁₅:0.015Tm³⁺,0.08Dy³⁺,0.02Eu³⁺ along with various temperatures

Value of x	Color coordinates			(ΔE)×10 ⁻³
	X	Y	D _{uv}	
300 K	0.326	0.332	-0.002	0.00
350 K	0.324	0.333	+0.002	6.97
400 K	0.322	0.334	-0.002	7.61
450 K	0.320	0.336	+0.006	7.93
500 K	0.317	0.338	+0.010	10.74
550 K	0.315	0.341	+ 0.014	12.18